**Supplementary information for "Geodetic slip solution for the $M_w$=7.4 Champerico (Guatemala) earthquake of 07 November 2012"**

by A. P. Ellis, C. DeMets, P. Briole, E. Molina, O. Flores, J. Rivera, C. Lasserre, H. Lyon-Caen, and N. Lord

# 1 Summary

This supplementary document contains text, figures, and one table that augment the main document, including tests of synthetic data sets to determine how well the Guatemala GPS network can resolve slip along the subduction interface and descriptions of blind tests of the coseismic GPS offsets and coseismic slip solution presented in the main document.

# 2 Repeatability of coseismic offsets estimated at the GPS sites

As part of our analysis, a subset of the authors, hereafter referred to as Team 2, independently processed the raw GPS observations used for this analysis and estimated coseismic offsets to evaluate the reproducibility of the offsets (Table 1) that were used for the main analysis. Team 2 processed the raw observations with GIPSY software and standard point-positioning procedures and estimated coseismic offsets at each site by fitting each station position time series with an equation that incorporated an instantaneous offset the day of the earthquake, linear motion before the earthquake, exponentially-decaying postseismic deformation, and a sinusoidal term to remove seasonal variations. Encouragingly, a comparison of the coseismic offsets from the primary analysis (Table 1 of the main document) to the alternative estimates (Fig. 1 and Table S1) yields similar offsets at most of the sites.

Team 2 also estimated offsets at seven campaign sites that were not included in the primary analysis (Supplemental Table 1). The offsets at the campaign sites were estimated by extrapolating site positions determined from campaign measurements that were variously made in 1999, 2003, and/or 2006 forward to the time of the 2012 earthquake and determining the offset between that extrapolated location and the location measured after the earthquake. Measurements at these seven sites after the earthquake did not occur until two weeks to six months after the earthquake. The coseismic offsets for the seven campaign sites thus include some postseismic deformation. Offsets at the seven campaign sites are shown in Fig. 1 below.

# 3 Robustness of the coseismic slip solution

As described in Section 4.2 of the main document, we also did a blind comparison of coseismic slip solutions determined from the preferred and alternative coseismic offsets. Fig. 2 compares the solutions determined from the two sets of coseismic offsets. As is described in Section 4.2 of the main document, the major features of the two solutions agree well despite the independent approaches that were used both determine their underlying coseismic GPS offsets and estimate the two solutions. We conclude that the geodetic solutions are robust. Readers are referred to Section 4.2 of the main document for further information.

# 4 Resolution of coseismic slip from synthetic slip solutions

Section 4.3 of the main document describes a series of tests that we used to determine how well the location and magnitude of coseismic slip can be resolved on the Middle America subduction interface from synthetic offsets at the locations of the 19 GPS sites that recorded coseismic slip for the 2012 Champerico earthquake. Figs. 3-5 show seven hypothetical distributions of coseismic slip that we imposed on an elastic half space to determine 3-D elastic displacements at each of the 19 GPS sites that recorded coseismic slip for the 2012 Champerico earthquake. The slip imposed along each fault patch consists of one meter of downdip motion uniformly distributed along the fault. The displacements predicted at the 19 GPS sites were inverted using the method described in the text to find a best-fitting slip solution for each of the seven starting models. In the absence of any noise in the synthetic displacements, the starting slip solutions were recovered perfectly (Figs. S3, panels B2 to F2). We simulated more realistic data by adding Gaussian noise to the synthetic displacements (Section 4.3). Inversions of the noisy synthetic displacements also correctly recovered the locations of the fault patches and slip magnitudes for depths between 10-60 km (Figs. S3, panels B3 to F3) to within 15% of their starting values. Concentrated slip imposed above 10 km was instead recovered as diffuse amplitude slip between 0-20 km (Fig S3, panel A3). Our ability to resolve shallow slip is thus limited.

The outcome of the synthetic tests indicates that the onshore GPS network has sufficient geometric strength with respect to a range of plausible offshore rupture locations to reliably recover the location and magnitude of the slip.

### References

Ye, L., T. Lay, and H. Kanamori, 2013. Large earthquake rupture process variations on the Middle America megathrust, *Earth Planet. Sci. Lett., 381*, 147–155, doi: 10.1016/j.epsl.2013.08.042.

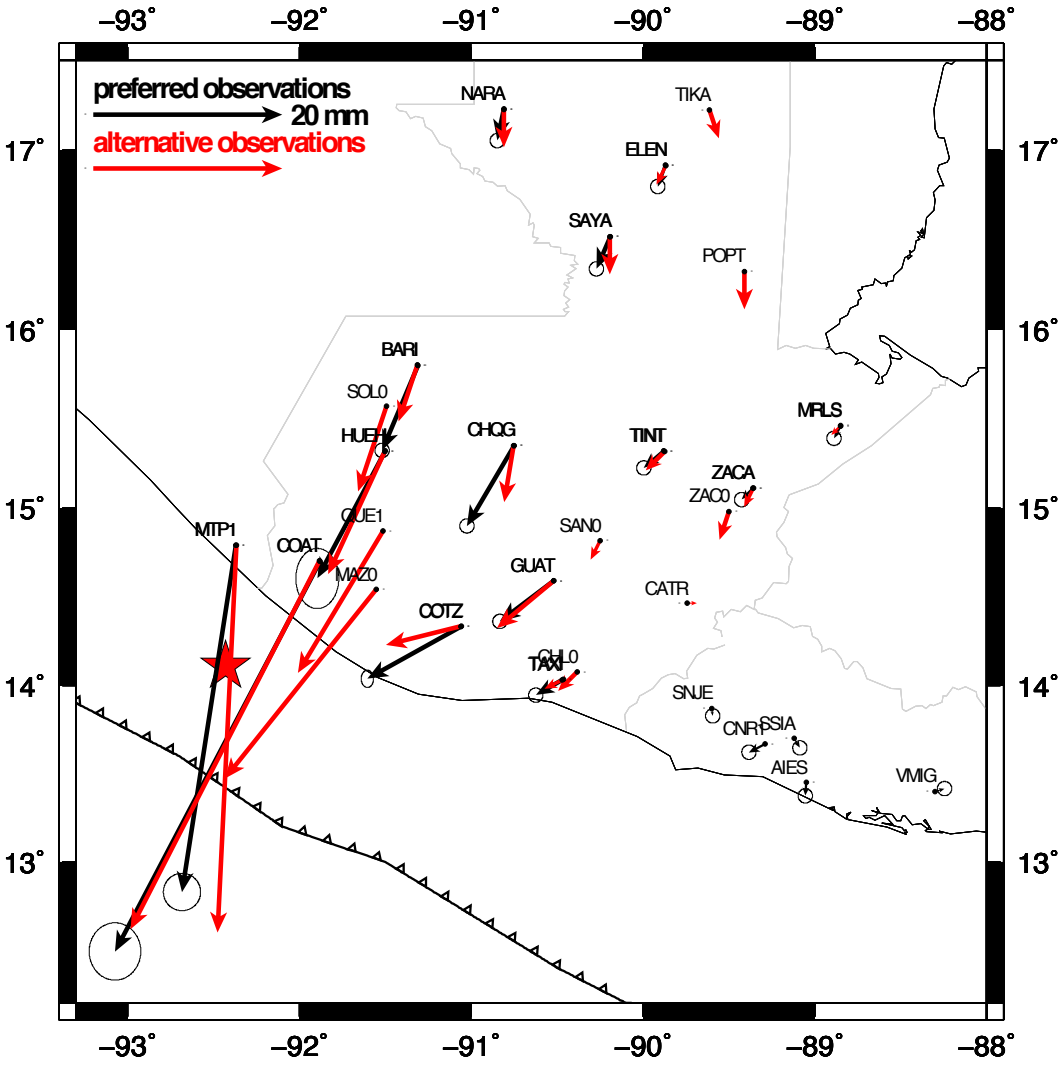


Figure 1: Comparison of coseismic offsets for the Champerico earthquake from the primary analysis (black arrows and Table 1) and the alternative analysis (red arrows and Table S1).

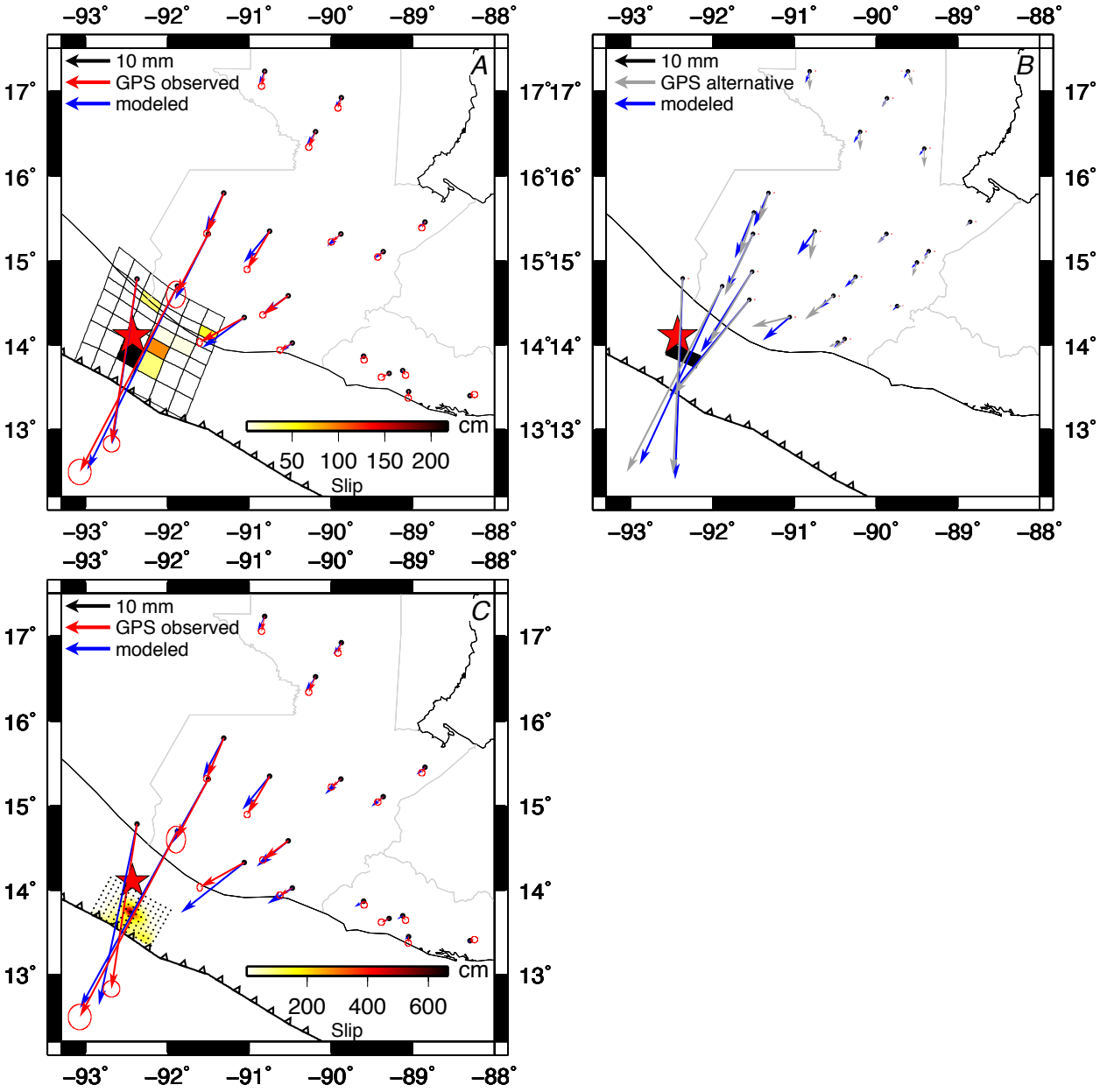


Figure 2: Measured horizontal coseismic offsets and predictions of three solutions for the coseismic slip. (A) - the preferred geodetic solution (Fig. 5a and Table 1 from the main document). (B) Alternative geodetic solution with ∼2.8 m of slip on a single fault. (C) Seismologically-derived slip solution of Ye et al. (2013) after translating the solution 51 km to the west from the solution location indicated by Ye et al. (2013).

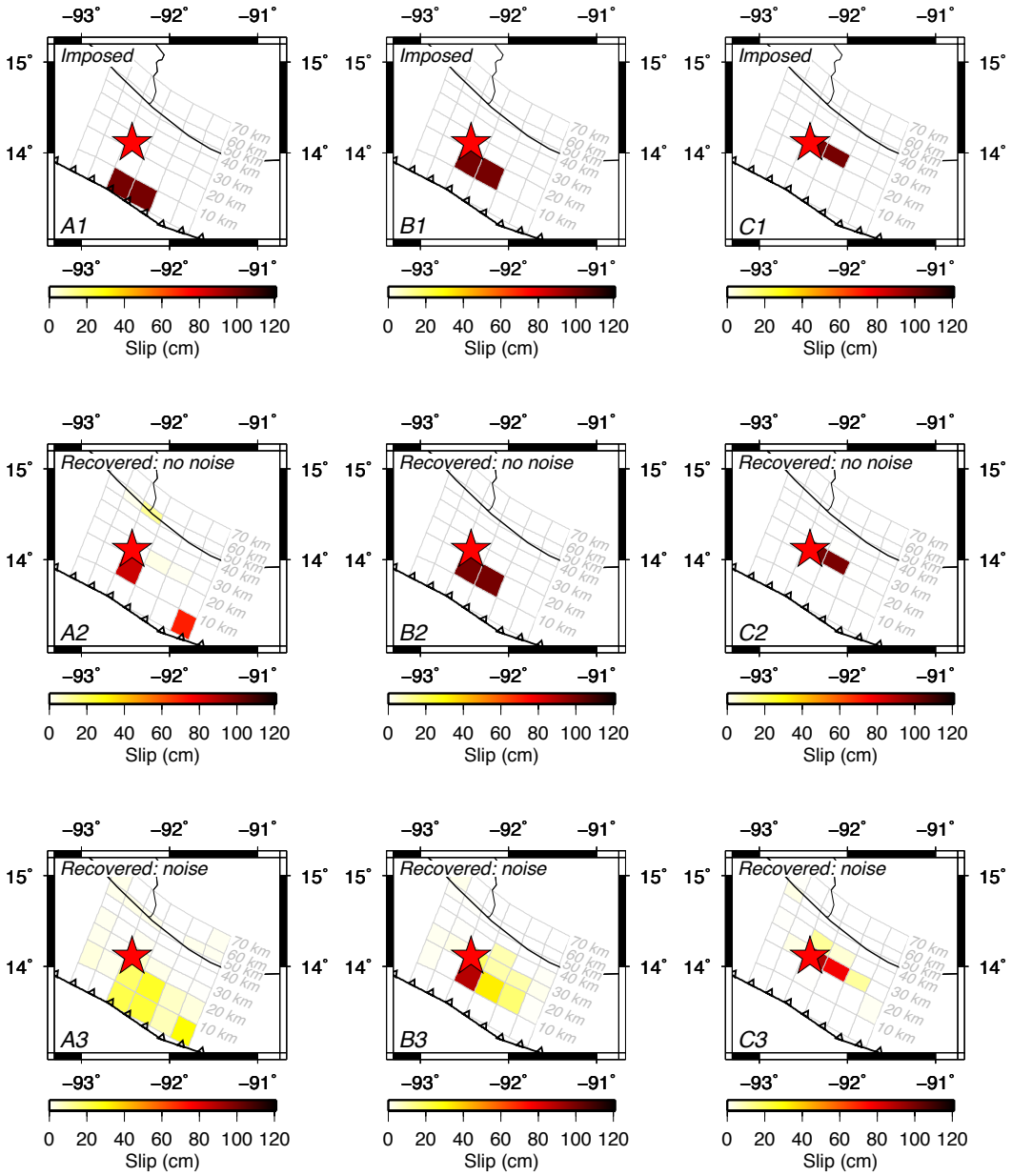


Figure 3: Results from slip-patch resolution test. Colored squares show fault patches where 1-meter of slip is either imposed (Panels A1-G1) or slip is estimated via inversions of synthetic coseismic offsets created with the imposed solutions (Panels A2-G2 and A3-G3). Red star indicates the epicenter of the 2012 Champerico earthquake. Further details are given in the main and supplementary documents.

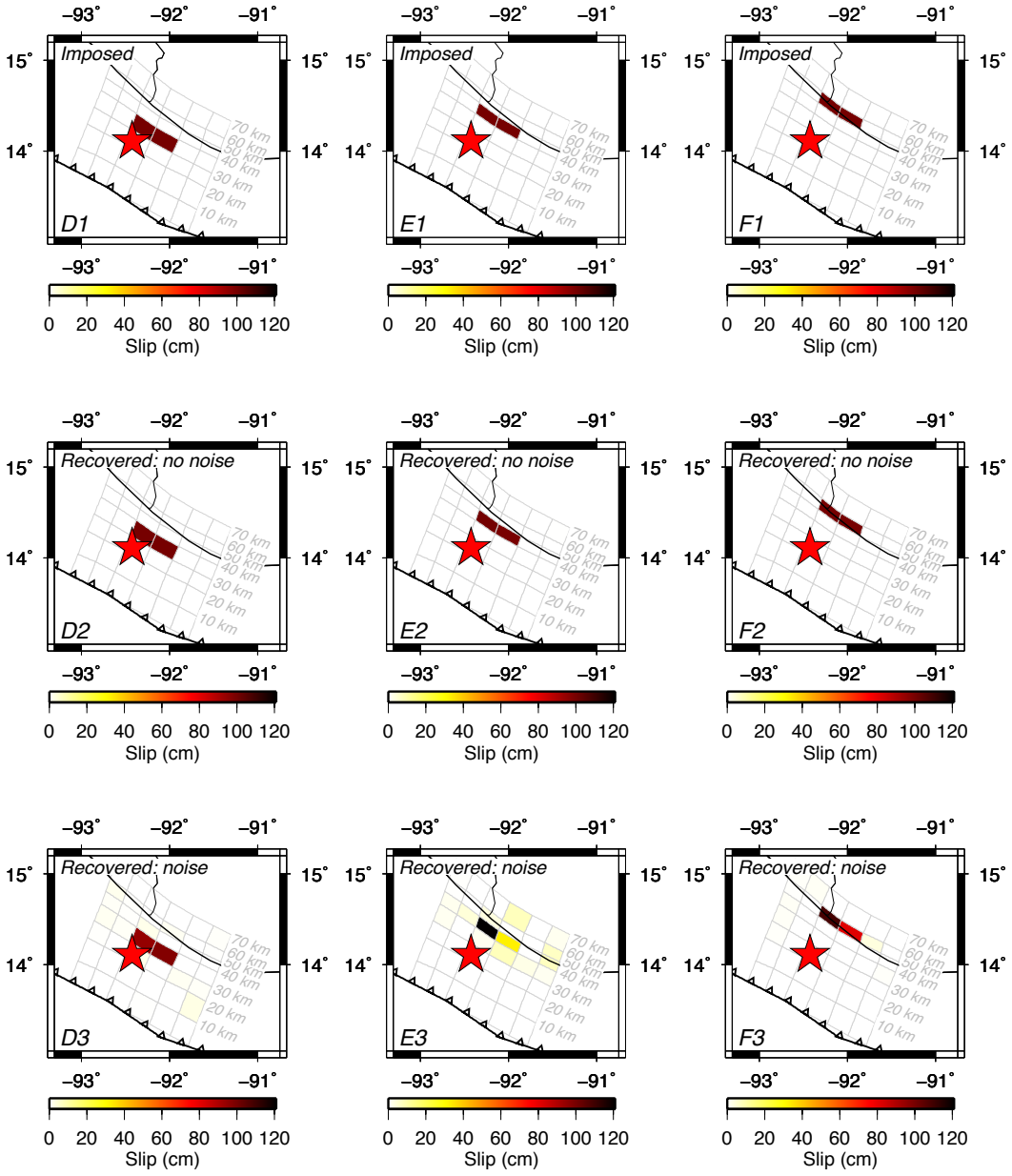


Figure 4: See caption to Fig. 3.

.

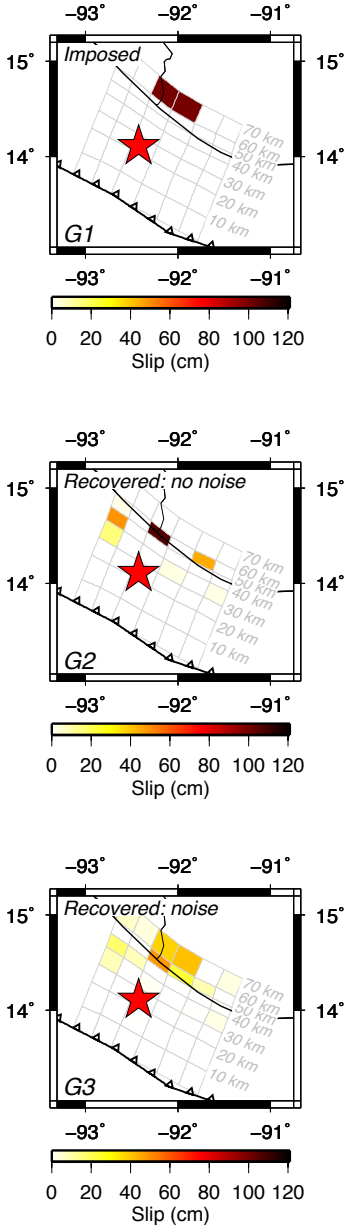


Figure 5: See caption to Fig. 3.

.

| Site Information | | | | Preferred Solution | | | | | | | | | Alternative Solution | | | |
|---|---|---|---|---|---|---|---|---|---|---|---|---|---|---|---|---|
| | | | | East (mm) | | | North (mm) | | | Vertical (mm) | | | East (mm) | | North (mm) | |
| *Site* | *Lat °N* | *Lon °E* | *Height (m)* | $Obs_e$ | $Model_e$ | $\pm 1\sigma$ | $Obs_n$ | $Model_n$ | $\pm 1\sigma$ | $Obs_v$ | $Model_v$ | $\pm 1\sigma$ | $Obs_e$ | $Model_e$ | $Obs_n$ | $Model_n$ |
| AIES | 13.447 | -89.050 | 35.82 | -2.1 | -0.3 | 0.5 | -7.3 | -0.3 | 0.5 | 2.0 | -0.5 | 2.0 | ----- | ----- | ----- | ----- |
| BARI | 15.802 | -91.315 | 1459.13 | -3.8 | -4.1 | 0.5 | -9.0 | -8.6 | 0.5 | -1.9 | 0.1 | 2.0 | -2.0 | -3.1 | -6.0 | -7.1 |
| CATR | 14.463 | -89.743 | 686.07 | ----- | ----- | ----- | ----- | ----- | ----- | ----- | ----- | ----- | 1.0 | -1.0 | 0.0 | -1.0 |
| CHL0* | 14.075 | -90.382 | 228.76 | ----- | ----- | ----- | ----- | ----- | ----- | ----- | ----- | ----- | -2.0 | -0.9 | -2.0 | -1.1 |
| CHQG | 15.350 | -90.752 | 1278.40 | -5.0 | -5.8 | 0.5 | -8.5 | -7.0 | 0.5 | -5.1 | -0.2 | 1.1 | -1.0 | -3.7 | -6.0 | -5.0 |
| CNR1 | 13.670 | -89.289 | 924.44 | -1.7 | -0.5 | 0.5 | -0.9 | -0.4 | 0.5 | -2.0 | -0.6 | 2.0 | ----- | ----- | ----- | ----- |
| COAT | 14.702 | -91.885 | 425.96 | -21.7 | -20.1 | 1.8 | -41.3 | -40.9 | 2.0 | 1.8 | -3.5 | 2.0 | -20.0 | -17.3 | -39.0 | -37.4 |
| COTZ | 14.335 | -91.058 | 302.24 | -9.9 | -9.4 | 1.3 | -5.5 | -6.7 | 2.0 | 1.5 | -0.5 | 7.6 | -8.0 | -5.7 | -2.0 | -4.9 |
| ELEN | 16.916 | -89.868 | 116.02 | -0.8 | -1.5 | 0.5 | -2.3 | -2.2 | 0.5 | -4.4 | 0.2 | 2.0 | -1.0 | -1.0 | -2.0 | -1.8 |
| GUAT | 14.590 | -90.520 | 1519.87 | -5.7 | -5.7 | 0.5 | -4.3 | -4.1 | 0.5 | 0.8 | -0.8 | 2.0 | -6.0 | -2.9 | -5.0 | -2.7 |
| HUEH | 15.328 | -91.503 | 1874.88 | -7.2 | -7.4 | 1.5 | -13.5 | -14.7 | 2.1 | -1.9 | -0.7 | 5.9 | -6.0 | -5.7 | -13.0 | -12.0 |
| MAZ0* | 14.537 | -91.550 | 342.00 | ----- | ----- | ----- | ----- | ----- | ----- | ----- | ----- | ----- | -16.0 | -16.8 | -20.0 | -20.2 |
| MRLS | 15.462 | -88.850 | 44.15 | -0.7 | -1.5 | 0.5 | -1.3 | -1.2 | 0.5 | -4.2 | 0.0 | 2.0 | -1.0 | -0.8 | -1.0 | -0.8 |
| MTP1 | 14.791 | -92.368 | 52.70 | -5.7 | -5.5 | 1.3 | -36.7 | -36.8 | 1.3 | 4.3 | -1.0 | 7.0 | -2.0 | -1.6 | -41.0 | -42.2 |
| NARA | 17.228 | -90.810 | 71.31 | -0.7 | -1.3 | 0.5 | -3.3 | -2.8 | 0.5 | 3.3 | 0.3 | 2.0 | 0.0 | -0.9 | -4.0 | -2.5 |
| POPT | 16.325 | -89.411 | 519.52 | ----- | ----- | ----- | ----- | ----- | ----- | ----- | ----- | ----- | 0.0 | -1.1 | -4.0 | -1.5 |
| QUE1* | 14.871 | -91.515 | 2386.53 | ----- | ----- | ----- | ----- | ----- | ----- | ----- | ----- | ----- | -9.0 | -10.8 | -15.0 | -17.0 |
| SAN0* | 14.816 | -90.249 | 994.43 | ----- | ----- | ----- | ----- | ----- | ----- | ----- | ----- | ----- | -1.0 | -2.3 | -2.0 | -2.3 |
| SAYA | 16.520 | -90.192 | 141.85 | -1.5 | -2.0 | 0.5 | -3.4 | -3.0 | 0.5 | -0.3 | 0.3 | 2.0 | 0.0 | -1.4 | -4.0 | -2.4 |
| SNJE | 13.868 | -89.601 | 1656.96 | -1.8 | -0.9 | 0.5 | -4.3 | -0.7 | 0.5 | 6.2 | -0.6 | 2.0 | ----- | ----- | ----- | ----- |
| SOL0* | 15.571 | -91.494 | 3356.79 | ----- | ----- | ----- | ----- | ----- | ----- | ----- | ----- | ----- | -3.0 | -4.0 | -9.0 | -9.6 |
| SSIA | 13.697 | -89.117 | 624.39 | 0.6 | -0.5 | 0.5 | -1.0 | -0.4 | 0.5 | -5.7 | -0.5 | 2.0 | ----- | ----- | ----- | ----- |
| TAXI | 14.035 | -90.465 | 45.02 | -2.8 | -2.2 | 0.5 | -1.6 | -1.8 | 0.5 | 0.5 | -0.9 | 2.0 | -2.0 | -0.8 | -1.0 | -1.1 |
| TIKA | 17.225 | -89.612 | 237.84 | ----- | ----- | ----- | ----- | ----- | ----- | ----- | ----- | ----- | 1.0 | -0.9 | -3.0 | -1.5 |
| TINT | 15.318 | -89.875 | 114.61 | -2.1 | -3.1 | 0.5 | -1.8 | -2.7 | 0.5 | -3.1 | 0.0 | 2.0 | -2.0 | -1.8 | -2.0 | -1.9 |
| VMIG | 13.396 | -88.305 | 374.85 | -1.8 | -0.2 | 0.5 | -6.3 | -0.2 | 0.5 | 2.2 | -0.3 | 2.0 | ----- | ----- | ----- | ----- |
| ZAC0* | 14.981 | -89.501 | 303.94 | ----- | ----- | ----- | ----- | ----- | ----- | ----- | ----- | ----- | -1.0 | -1.2 | -3.0 | -1.2 |
| ZACA | 15.113 | -89.356 | 130.31 | -1.2 | -2.0 | 0.5 | -1.2 | -1.6 | 0.5 | -1.5 | -0.1 | 2.0 | -1.0 | -1.1 | -2.0 | -1.1 |

*Denotes campaign station

Table S1: Coseismic observed offsets and estimated offsets from preferred and alternative solutions described in main document.